

Experimental and Numerical Analyses of the Temperature Field in the Ironing Process

Vesna MANDIĆ*, Dragan ADAMOVIĆ, Zoran JURKOVIĆ, Marko DELIĆ

Abstract: The purpose of this paper is to determine the temperature fields in the workpiece and the tool in the ironing process using an integrated approach that includes laboratory experiments and numerical modelling. An originally developed model device for ironing sheet metal strips, which was previously shaped by U-bending, was used for the experimental research. Thermocouples were installed in the device at the position close to the contact surface with the workpiece. The device was mounted on a hydraulic press that enables maximum ironing speeds of $v = 4,17$ mm/s. In order to determine the temperature fields at higher ironing speeds, a series of numerical experiments was performed at identical speeds as in the experiments (0,33 mm/s and 4,17 mm/s) and at higher speeds (100 mm/s, 1000 mm/s and 10000 mm/s). Good matches of the experimental and numerical results at lower speeds were obtained, so the numerical estimates at higher speeds were valid for the analysis and conclusions. With the increase of the ironing speed, a trend of temperature increase is evident. The maximum temperature of 166 °C at ironing speed of 10000 mm/s that corresponds to manufacturing of 250 cans per minute is significantly lower than the critical melting temperature of the tin coating.

Keywords: finite element method; ironing; numerical simulation; physical modelling; temperature

1 INTRODUCTION

Tribological conditions in the metal forming and, especially, in ironing depend to a large extent on the pressure in the contact zone between the tool and the workpiece, the material and the roughness of the surfaces in contact, as well as the length of the sliding zone and the sliding speed. However, the combination of the mentioned parameters indirectly affects the temperature increase in the interface and consequently the performance of the lubricant. Measuring interface temperature is not easy, especially in industrial ironing processes. Temperature measurements performed by Stolte [1] have shown that the temperature at the direct contact points amounts to 970 °C. Barber [2] has concluded, based on microscopic observations of the structure changes, that the temperature reaches values of 1000 °C. Due to the plastic deformation of material and friction between the ironed material and tool, an increase of temperature occurs, especially at higher ironing speeds. Increased temperature within the interface can significantly influence changes of the lubricant's characteristics, through the change of the lubricant's viscosity. Also, the increased temperature can intensify the tool wear process. In ironing the tin coated thin sheets, temperature significantly influences the state of the tin coating. Due to the aforementioned reasons, it is necessary to take into account the generated heat at the interface, especially at the higher ironing speeds, and enable its conducting away from the contact by the lubricant, which, at the same time, plays the coolant's role [3]. Research dealing with these problems is mainly related to high-speed ironing processes. Authors of the paper [4] investigated the determination of the interface temperature in an industrial ironing process. It has been shown that under extreme ironing conditions it can lead to lubricant film breakdown and galling, after several strokes. Experimental measurements of the tool temperature in a few points at thermal steady-state of the process were realized in order to define appropriate boundary conditions for finite element simulations. The results showed that the frictional heating is the primary cause for the peak temperature (158 °C during the forward stroke and 150 °C during the backward stroke), as the friction coefficient in numerical

simulation has a large influence on the interface temperature. On the other hand, the heat transfer coefficient for the tool material has no practical effect when the process is already in steady-state. For the food and beverage cans, thin steel sheets with the tin coating (white thin sheets) are used in the ironing process. The melting temperature of tin is 323 °C and it is very important that this temperature is not exceeded during the process. In the opposite case, if this temperature is exceeded, the larger roughness of the surface would appear what would disrupt the forming process. Also, temperature increase can lead to the failure of the tin coating layer continuity and such a can would be useless [5]. Djordjevic et al. [6] investigated the contact pressure in the deep drawing of the Al thin sheet using the tribological model of the strip sliding in the flat die on the device developed by Adamovic [7]. The multi-factor experiment was performed with the contact elements of various roughnesses, with different lubricants and variable contact pressure. The goal was to examine different mathematical models of the dependence of the contact pressure in the course of the sliding strip. Satisfactory matches of the defined mathematical models for estimating the contact pressure depending on the mentioned variables with the experimentally obtained results were obtained. It is not often possible to experimentally measure temperatures and working pressures directly at the interface. Therefore, many researchers apply the thermo-mechanically coupled finite element (FE) simulations for estimates of the temperature and pressure distributions in the contact between the tool and the workpiece in ironing. Kim et al. [8] performed a series of FE numerical simulations of the tribo-tests during ironing to establish the influence of lubricant on the temperature and pressure distributions in the contact. They varied the values of coefficients and factors of friction until the satisfying agreement was reached between the force diagrams obtained by experimental measurements of the force on the punch and numerically estimated ones. With such an inverse procedure, the parameters of friction were determined for various lubricants as well as their influence on pressures and temperatures in the contact and consequently the tool wear and galling. In a similar investigation [9], the calibration curves were obtained by

FE analyses of ironing force for various values of the friction factor (from $m = 0,05$ to $m = 1$) in the contact at environmental temperatures of $T = 20\text{ }^{\circ}\text{C}$ and $T = 100\text{ }^{\circ}\text{C}$. From the calibration curves and experimentally obtained force diagrams, one can estimate the friction factor for any applied lubricant as well as its applicability for ironing. Han et al. [10] investigated deep drawing and three-stage wall ironing process as nonlinear and coupled thermo-mechanical contact problem with axisymmetric non-isothermal FE analysis, for better understanding of the heat generation from deformation heating and friction heating, as well as the heat dissipation from conduction and convection. A lot of information was obtained from this analysis, which was compared and confirmed with experimental research utilizing a pilot can making line. It was observed that the temperature rises more significantly in the ironing process than in deep drawing, due to the greater length of punch sliding and thickness reduction ratio. Thus, in the third ironing operation, a peak of $320\text{ }^{\circ}\text{C}$ was reached, which is much higher than the melting point of the surface tin of tinplate. The influence of temperature on the characteristics of the final product manufactured, among other things, by the ironing operation at higher sheet temperatures was investigated using explicit finite element code LS-DYNA in the study [11]. The obtained results were in good agreement with the experiments. Authors of this paper, in their earlier studies, carried out extensive research on sheet metal forming in deep drawing and ironing processes [7, 12, 13]. In addition to complex multifactorial experiments on special model devices, research was also carried out using numerical simulations based on the finite element method, through a combined experimental-numerical approach [14]. The main aim of the coupled thermo-mechanical analyses in this paper is to gain understanding of the heat development and its conduction in the contact for the high ironing speeds that were not possible to be investigated by physical experiments.

2 EXPERIMENTAL SETUP

Experimental research was carried out on the original device for modelling the ironing process in laboratory conditions [7]. On this device, it is possible to vary the geometric and physical conditions of the real ironing process, such as different materials of the die and the punch, the roughness of the contact surfaces, the die angle and the ironing speed. The device was installed on the universal laboratory machine for sheet metal testing ERICHSEN 142/12 and placed in the frame of the tensile fixture (Fig. 1). The main drive of the machine was used for the main action of the ironing force, and the lateral pressure on the dies, and thus on the wall of the tested specimen, was achieved by means of a cylinder driven hydraulically via a separate pump. The tests were carried out by placing the sheet metal strip, subjected to U-bending beforehand, on the "punch" 3, and then, when modelling the ironing process, it was acted upon by force F_D by "dies" 2. The dies were placed in supports 1, where the left support was stationary and the right one was movable together with the right die. The sheet metal strip was ironed between the dies under the influence of the force acting on the punch front 4. Due to the action of the force F_D , the

wall thickness of the sheet metal strip was reduced, which on the one side, slides on the surfaces of the dies 2 inclined at angle α , and on the other side on the surfaces of the punch plates 6. The dies 2 and the punch plates 6 can be made of different materials. Their roughness and also die slope angles α can be different.

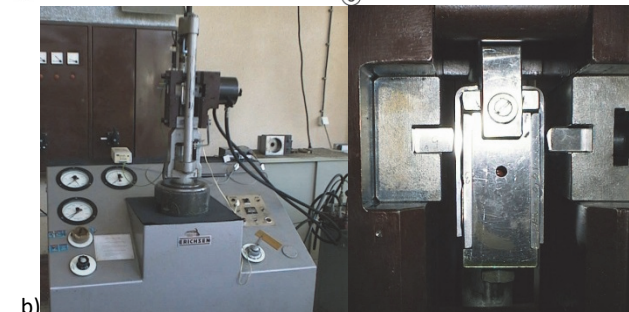
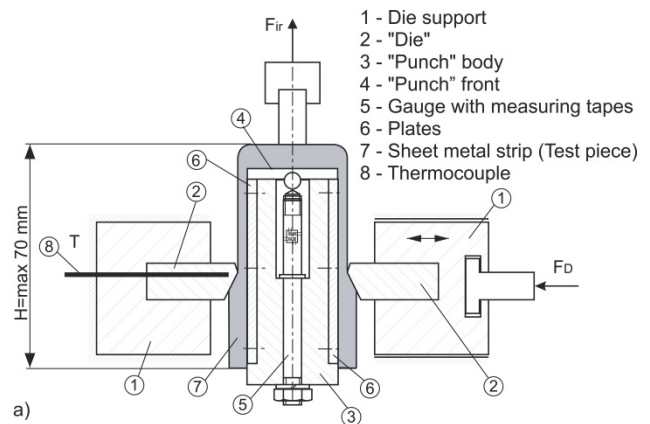


Figure 1 Strip ironing device: scheme (a) and mounted on hydraulic press (b)

For temperature measurement, a type K (nickel-alumel) of thermocouple was used, with a measurement range from -200 to $1250\text{ }^{\circ}\text{C}$, and it was placed in a drilled hole through the device's body, the die support as well as the die itself. The hole through the die was made with a flat bottom, in order to achieve good contact between the tip of the thermocouple and the die. The distance between the hole bottom and die's radius was $0,3\text{ mm}$. The signal obtained from the thermocouple was amplified and then taken to the AD converter. Fig. 2 shows the placement of the thermocouple in the modelling device. The test strips were made of low-carbon sheet steel DC04, designed for metal forming processes. The tested steel sheet had properties prescribed by the SRPS EN 10130:2004 standard. Dies and punch plates were made of alloyed tool steel (TS) marked according to EN as X160 CrMoV 12 1. Die and punch surfaces were polished. The dimensions of the bent workpiece and some of them after the strip ironing model process are shown in Fig. 3.

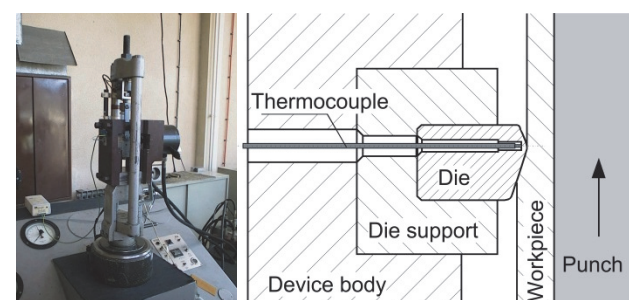


Figure 2 Placing of the thermocouple for temperature measurements

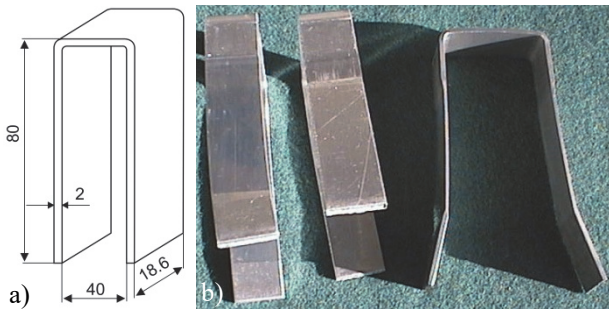


Figure 3 Specimen dimensions (a) and strips after ironing (b)

Tab. 1 provides other data important for the conducted experimental research, which relate to the material properties of the workpiece and tools, properties of contact surfaces, as well as varied process parameters.

Table 1 Material and surface properties and experimental conditions

		Material	Mechanical properties	Surface properties
Die and punch plate		Tool steel (TS) X165CrMoV12	Hardness 60 ÷ 63 HRC	$R_a \approx 0,01 \mu\text{m}$ (N1)
Workpiece		DC04 Thickness: 2,0 mm Width: 18,6 mm	$R_p = 186 \text{ MPa}$ $R_m = 283 \text{ MPa}$ $A_{80} = 37,3 \%$ $n = 0,2186$ $r = 1,09009$	$R_a = 0,92 \mu\text{m}$ $R_p = 3,62 \mu\text{m}$ $R_v = 5,11 \mu\text{m}$
Reduction degree: 3,5 ÷ 24%		Angle of die gradient: $\alpha = 20^\circ$		
Sliding path: max 70 mm		Temperature: room temperature		
Ironing speed: 20 mm/min (0,33 mm/s); 250 mm/min (4,17 mm/s)		Strip holding force (F_D): 8,7 kN; 17,4 kN; 26,1 kN		
Applied lubricants	On die side	L1 - Lithium grease with additive of the molybdenum disulphide (Li+MoS ₂) - Grease		
	On punch side	L2 - Non-emulsifying mineral oil with mild EP qualities - Oil ($v = 45 \text{ mm}^2/\text{s}$)		

3 NUMERICAL MODEL

A series of numerical experiments, using the finite element method and specialized Simufact. forming software for the simulation and analysis of the metal forming processes [15], was conducted with the aim of investigating the temperature fields in the workpiece and the tool during the ironing process. Heat generation due to plastic deformation and contact friction and its transfer from the workpiece to the die and environment were determined. The same levels of influential process parameters were used in numerical experiments as in laboratory experiments (Tab. 1), with the exception of the ironing speed. Two of them had the same ironing speeds (0,33 mm/s and 4,17 mm/s), while three numerical experiments were carried out with higher speeds in order to illustrate their influence on distribution of temperature in workpiece and dies (100 mm/s, 1000 mm/s and 10000 mm/s). The enhanced version of the MARC finite element solver was used, based on the displacement method and the coupled thermal-mechanical approach, was used. The constitutive relations for this coupled approach are defined by the matrix Eq. (1) and Eq. (2):

$$K(T)u = f \tag{1}$$

$$C(T)\dot{T} + k(T)T = Q + Q^1 \tag{2}$$

where K is the system stiffness matrix, u is the nodal displacement, f is the force vector, C is the heat capacity matrix, T is the nodal temperature vector, \dot{T} is the time derivative of the temperature, k is thermal-conductivity matrix, Q is the thermal load vector (flux) and Q^1 is the internal heat generated due to plastic deformation. K , k and C are all temperature dependant.

In a coupled thermo-mechanical numerical simulation, the critical input parameters are heat properties of workpiece and tools, initial temperatures, heat transfer and emissivity parameters as well as friction properties for the interface. As numerical experiments rely on experimental data (Tab. 1), additional input data describing thermal processes are given in Tab. 2.

Table 2 Input thermal data for FE numerical simulations

Input data for FE simulations	Workpiece	Die
Initial temperature / °C	25	25
Thermal conductivity / W/m K	50	-
Specific heat capacity / J/kg K	478	-
Heat transfer coefficient to ambient / W/m ² K	50	77
Emissivity for heat radiation to ambient	0,25	0,25
Heat transfer coefficient to workpiece	-	6000

One of the most important input parameters for numerical simulations is the mathematical model that describes the plastic flow of the material during deformation. The workpiece is a strip of sheet metal DC04, which was cut in the direction of sheet rolling (0°), so the specimens were prepared in that direction for the standard tension test and determination of flow curve, i.e. the true stress - true strain relationship. The tests were performed in laboratory conditions ($v = 20 \text{ mm/min}$, $T = 20 \text{ }^\circ\text{C}$). The experimentally obtained curve was approximated in an exponential form (Eq. (3)), which was used to describe the plastic flow of the material in numerical experiments.

$$\sigma = 491,6874 \cdot \varphi^{0,2186} \tag{3}$$

The influence of contact friction is very significant in the ironing process, so these conditions must be precisely described in numerical experiments with an adequate mathematical model. A scheme of all the forces acting on the strip during the process is shown in Fig. 4. The principles of Coulomb's law were applied to describe the contact friction. In the laboratory experiments, the forces were measured by sensors, so that the friction coefficients (μ_p and μ_D) were calculated for the contact surfaces of the workpiece with punch and dies according to Eq. (4) and Eq. (5).

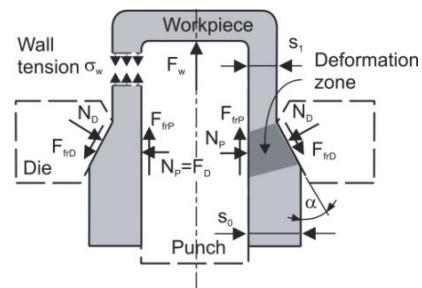


Figure 4 Scheme of forces acting during ironing process

$$\mu_p = \frac{F_{frP}}{2 \cdot F_D} \tag{4}$$

$$\mu_D = \frac{F \cdot \cos\alpha - 2 \cdot F_D \cdot \sin\alpha}{F \cdot \sin\alpha + F_D \cdot \cos\alpha} \tag{5}$$

In numerical experiments with higher ironing speeds, it was necessary to recalculate friction coefficients in accordance with results presented in the study [5]. Tab. 3 shows the applied values of friction coefficients for both contact surfaces and for all varied ironing speeds.

Table 3 Applied friction coefficients depending on ironing speed

Ironing speed / mm/s	μ_p		μ_D	
	% of change	Recalculated	% of change	Recalculated
0,33	0	0,1063	0	0,0707
4,17	+10% of 0,1063	0,1169	+10% of 0,0707	0,0777
100	-2% of 0,1169	0,1145	-2% of 0,0777	0,0761
1000	-3% of 0,1169	0,1133	-3% of 0,0777	0,0753
10000	-15% of 0,1169	0,0993	-15% of 0,0777	0,0660

Given that for the temperature field research experiments in the ironing process, specimens obtained through U-bending of the sheet metal strip (Fig. 3) were used, it was necessary to realize all the numerical experiments through modelling of two operations: the first operation as U-bending of the sheet metal strip to obtain specimens, the second one for modelling the ironing process. In this way, the previous history of U-bending was included in the analysis, so the virtual specimens were introduced into the ironing operation with residual stresses and plastic strains after the first forming operation. The geometry of the sheet metal strip (dimensions 200 × 20 × 2,01 mm) was modelled directly in *Simufact.forming* editor, while 3D CAD models of punch and dies were prepared in CATIA CAD software and imported into *Simufact.forming* as IGES files. For bottom calibration, an additional elastic tool was introduced between the two dies, which provides additional spring force and achieves a very small elastic springback effect. In multi-operation processes, when the deformation history is followed, it is important to include the effects of elastic recovery between operations [16, 17] in the FE simulation. For the first U-bending operation, initial finite element mesh was generated automatically in the workpiece using Sheetmeshmesher and hexahedral elements in two layers of thickness (element size 1 mm, number of FE elements was 7268).

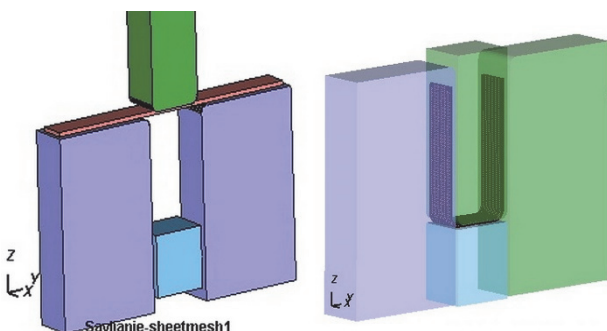


Figure 5 Numerical model of the bending process

Fig. 5 illustrates the model of bending process in *Simufact.forming* editor. Axial stress distributions before and after springback calculation, which has been performed automatically after bending numerical simulation, are presented in Fig. 6.

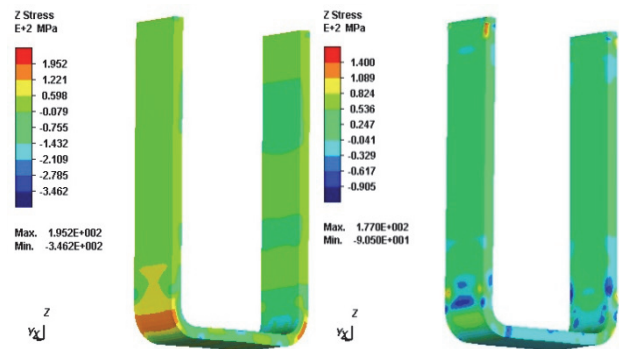


Figure 6 Axial stress distribution prior and after springback

For the numerical simulation of the second operation of the ironing process, a virtual model of the workpiece after the U-bending operation, with a complete deformation history, and after the calculated springback, was virtually placed on the punch model, symmetrically between dies. Distance between the dies defined the reduction of strip thickness, i.e. strain of the strip. Virtual workpiece and its position in the tool in the numerical model of ironing process are shown in Fig. 7.

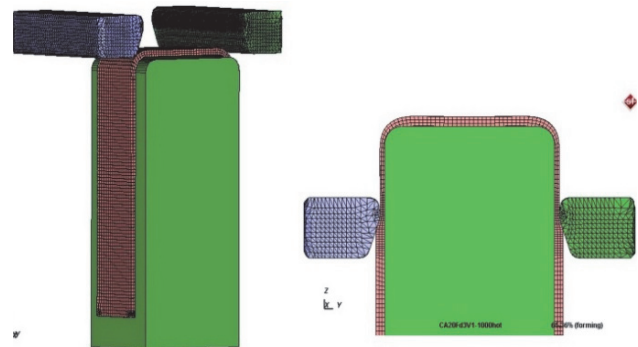


Figure 7 Numerical model of the ironing process

Sheetmesh mesher was used for remeshing bent strip in three layers per thickness. Total number of hexahedral elements was 10908 in the beginning of the simulation. In order to avoid simulation problems due to large distortion of initial mesh in the deformation zone during the ironing, remeshing criteria were defined (strain 0,4, element size 1 mm and two refinement boxes in contact zones close to dies). Overlay hex mesher was used for die meshing, with refinement box covering die angle zone. Total number of hexahedral elements of die was 6396.

4 EXPERIMENTAL AND NUMERICAL RESULTS

Despite the fact that the temperature in the contact zone varies with the change in ironing speed and holder forces (distances between dies, i.e. different thickness reductions), in experiments at low laboratory speeds ($v_{max} = 4.17$ mm/s), it was not possible to register larger temperature changes with direct temperature measurement via thermocouples placed in die near the contact surface.

Nevertheless, such measurements were necessary for defining boundary conditions for numerical experiments and their validation. Temperature was measured along the whole sliding path for each specimen. Dependence of the temperature variation on the sliding path for various ironing speeds and different holder forces (different strains) is shown in Fig. 8. Diagrams were obtained at ironing speeds (punch velocity) of 20 mm/min and 250 mm/min (0,33 mm/s and 4,17 mm/s, respectively).

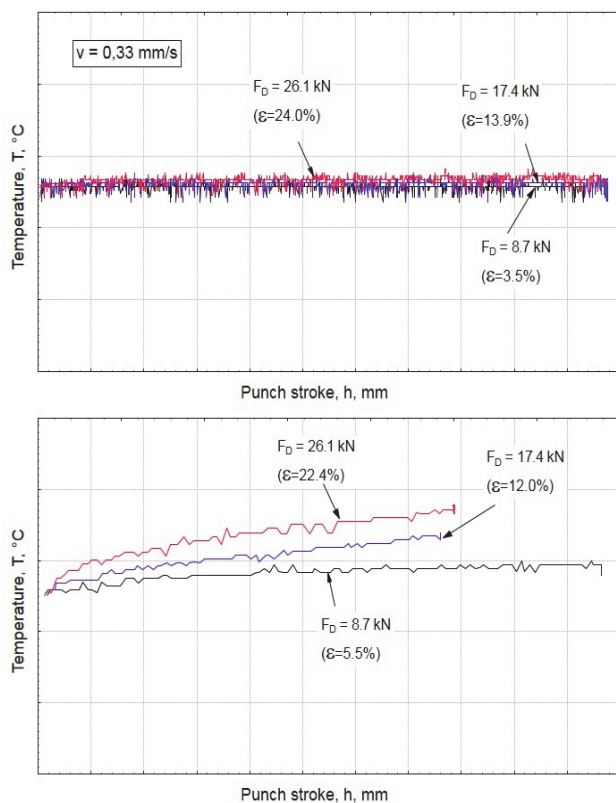


Figure 8 Temperature variation with punch stroke at different holder forces (strains), for ironing speeds of: 0,33 mm/s and 4,17 mm/s

At ironing speed of 0,33 mm/s, temperature increase along the corresponding sliding path was very small and it ranged within the limits of measurements error (± 1.5 °C). With ironing speed increase, the increase of temperature occurred as well. Also, with the increase of the strain at ironing speed of 4,17 mm/s somewhat higher increase of temperature was noticed. This temperature increase with respect to environment temperature (room temperature) was 4 °C to 12 °C where the lower temperatures corresponded to the lower strain (i.e. F_D). It was considered that the initial temperature, namely the environment temperature, which is exactly the temperature measured at the beginning of the experiment, was shown on diagram when the punch stroke is equal to zero. It should be emphasized that it was always taken care that enough time elapses between tests with different specimens, so that the punch temperature can be equalized with the temperature of the environment. Unlike the experiments, where it is possible to measure the temperature only at one point in the borehole in the matrix, close to the contact surface, in the numerical experiments, the temperature field is obtained in the entire volume of the die and the workpiece at the same time, under any conditions of performing the ironing process and in any arbitrary moment. The temperature

fields in the die and the workpiece derived by numerical model at ironing speed of $v = 0,33$ mm/s in different phases of the process (punch stroke $h = 3$ mm, 15 mm, 25 mm and 35 mm) is presented in Fig. 9. The generated heat in the workpiece, caused by plastic deformation and contact friction, is transferred in the contact zone to the die. When the ironing speed is low, the contact time is longer, so heat transfer occurs from the contact surface through the entire matrix. At the same time, the workpiece coming out of the die radius and the contact zone is then cooled due to heat radiation to the environment. From the initial 25 °C, the temperature inside the workpiece reached a maximum value of 27,6 °C, while in the die at a position 0,3 mm from the contact surface, as in the experimental measurements, the temperature reached a value of 26,6 °C. In a numerical experiment with the ironing speed of $v = 10000$ mm/s, which corresponds to an industrial process in the production of 250 cans per minute, the temperature fields were significantly different, as shown in Fig. 10. In comparison with the numerical experiment at the lowest ironing speed, at sliding path of 3 mm, the temperature in the workpiece in the contact zone reached a value of 97,5 °C. However, due to the high speed of the workpiece material passing through the die, there was no time for the generated heat to be transferred to the die. Heat transfer to the die is evident only with a sliding path of 15 mm. The maximum temperature reached in the workpiece was 166 °C and in the die at the thermocouple position was 133 °C. For the comparative analysis of temperature fields at different ironing speeds, only the results of numerical experiments at the maximum sliding path of 35 mm will be considered, because the maximum temperatures are reached at that moment. Fig. 11 shows the results of numerical simulations of the ironing process at speeds from 0,33 mm/s to 10000 mm/s, namely the temperature distribution in the entire workpiece and in one of the dies (on the left) and the development of the temperature field in the contact zone with indicated temperature values (on the right). Increasing the ironing speed leads to an increase of the temperature in the contact zone, and its transfer to the tool and radiation to the environment is less evident due to the short duration of the process. Such conditions and local heat development in small contact volumes are unfavourable for the workpiece and tin-coated sheets, as well as for the lifetime of the tool in contact. Lubricants and coolants for industrial processes must be chosen with special care because heat transfer to the tool and radiation to the environment is almost imperceptible at high speeds, as shown in Fig. 11.

Fig. 12 shows the trend of maximum temperature changes in the tool at the thermocouple position (finite element located at a distance of 0,3 mm from the matrix radius), at different ironing speeds. As the ironing speed increases, the heating of the dies becomes more intense. At a speed of 10000 mm/s and a sliding path of 35 mm, a temperature of 135 °C is reached at the reference point in just 3,5 μ s. With the use of adequate coolants and lubricants, a lower temperature in the tool can be expected. The trend of maximum temperatures in the workpiece at different ironing speeds, which were identified in direct contact with the die at the transition radius, is shown in the diagram in Fig. 13.

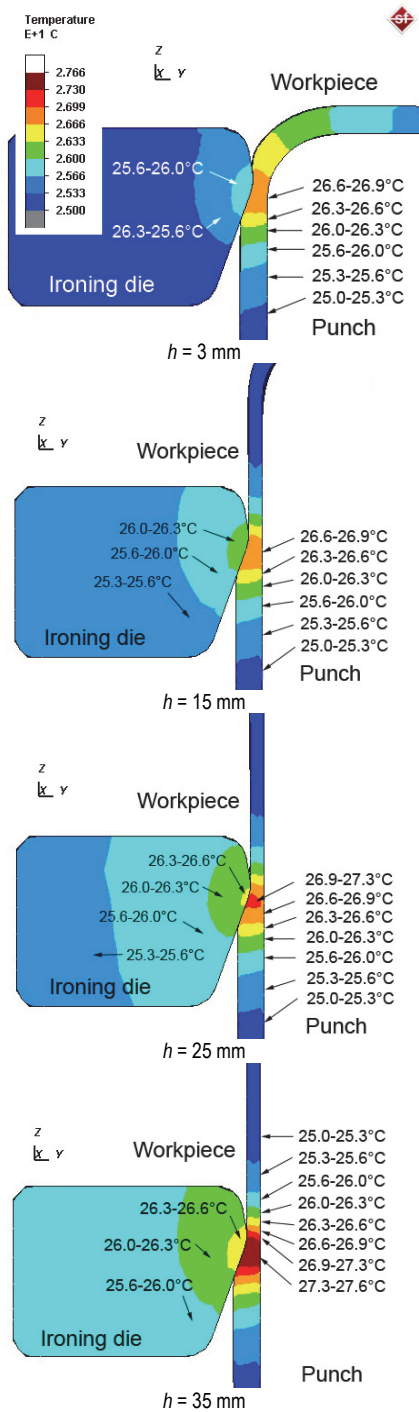


Figure 9 Temperature fields in contact zones at ironing speed of $v = 0,33$ mm/s

As opposed to the trend of the increase of the maximum temperatures in the die, the maximum values of the temperature in the workpiece were reached at sliding paths from 15 mm to 20 mm, depending on the ironing speed. Since the process is stationary after the strip passes through the dies, due to the same realized strain, strain rate and "numerically set constant value of the friction coefficient", such results were expected. However, each numerical experiment was realized with the initial temperature of the bent strip as workpiece and tool of 25 °C, which is not the case in real processes, despite the application of coolants. Thus, one can expect that numerically estimated values should be somewhat higher than those in the industrial manufacturing processes [5].

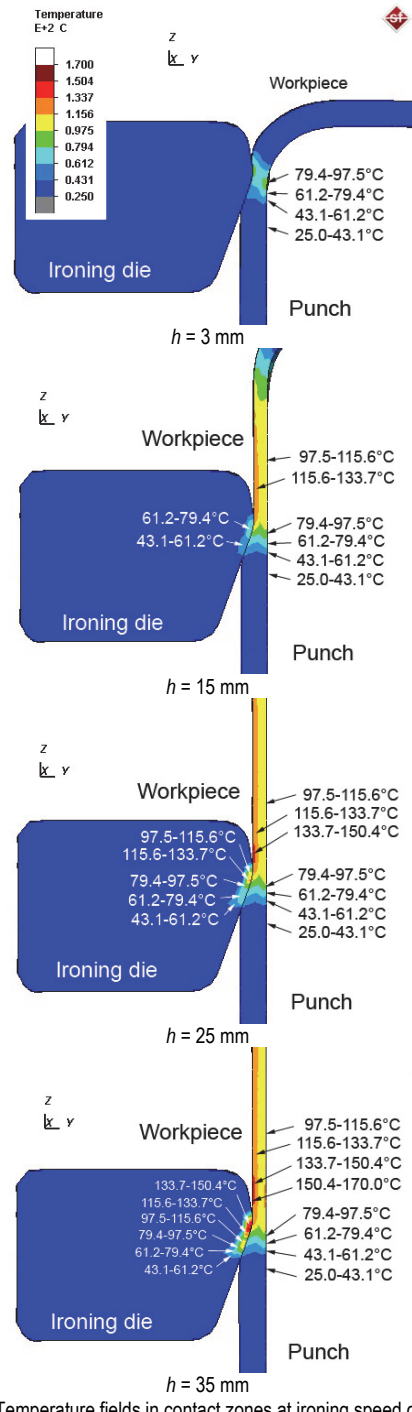


Figure 10 Temperature fields in contact zones at ironing speed of $v = 10000$ mm/s

The comparative diagram with the trends of the maximum temperatures in the die and the workpiece at all ironing speeds investigated by numerical and physical experiments is shown in Fig. 14. Although the workpiece and the die are in contact, no coincidence of the maximum temperatures can be expected considering that those in the die were measured at a thermocouple position 0,3 mm away from the die's radius, both in experiments and in the corresponding finite element in numerical simulations, at a given time.

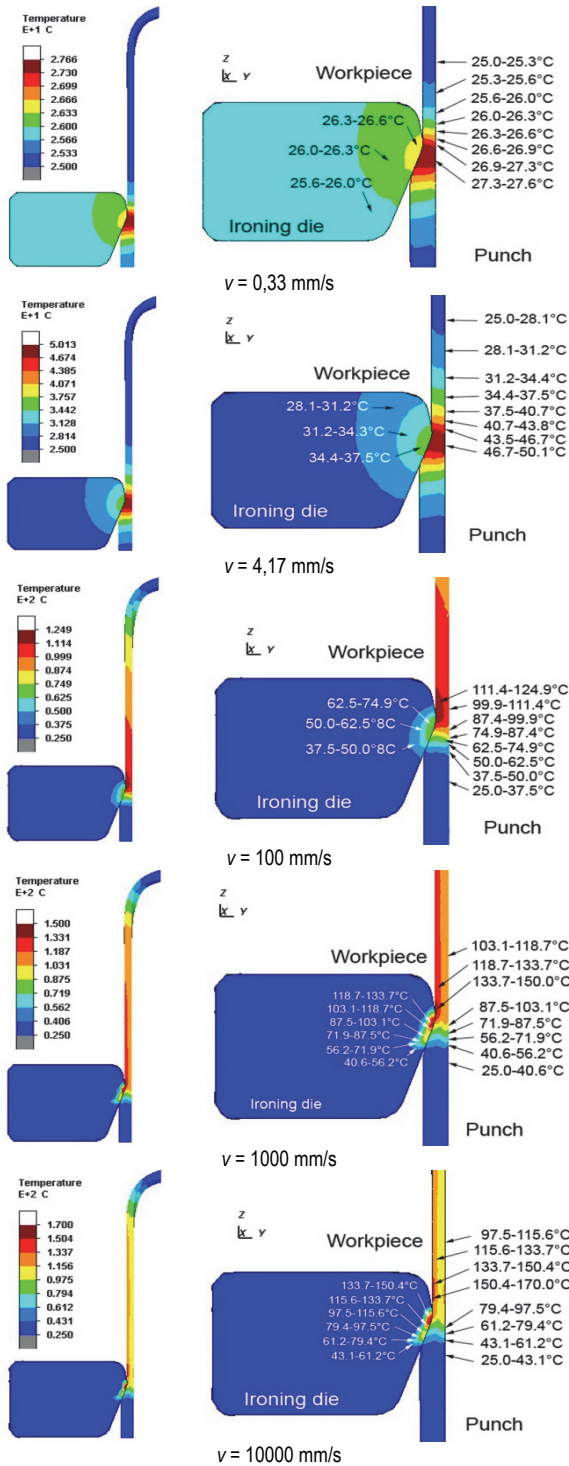


Figure 11 Temperature fields in the die and the workpiece at various ironing speeds

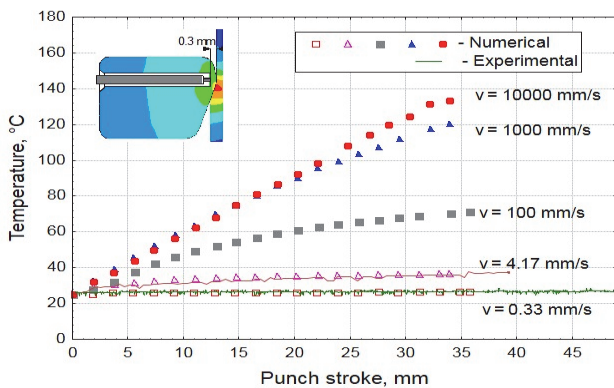


Figure 12 Temperature variation at the die

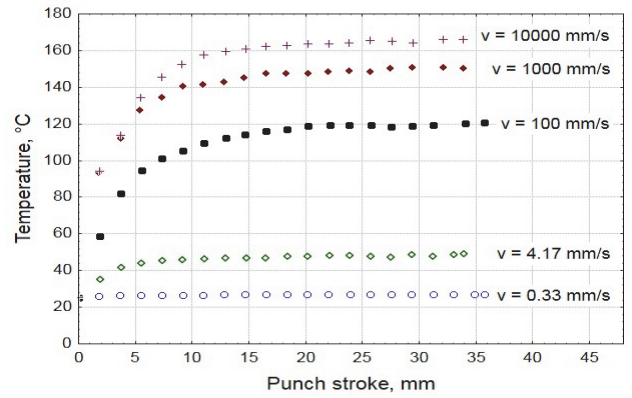


Figure 13 Temperature variation at the workpiece

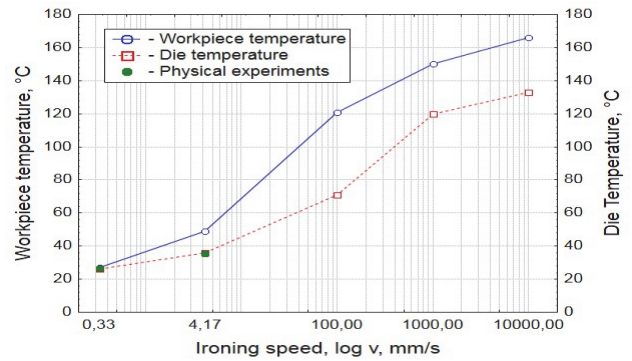


Figure 14 Maximum temperatures in the die and the workpiece (numerical and physical experiments)

5 CONCLUSION

This study aims at investigating the heat generation and its transfer in the interface between the workpiece and the tool at higher ironing speeds, which could not be applied in experimental research due to the limited speed ranges of the laboratory equipment, through a coupled thermo-mechanical finite element analysis of the ironing process. Due to the plastic deformation of the material and the friction between the workpiece and the tool, the temperature increases, especially at higher ironing speeds. The results of the present study revealed that at the same ironing speed, the highest temperature was obtained at the highest strip holding force, which corresponds to the highest strain. Also, at a constant holding force, with an increase in ironing speed, the temperature also increases. The established trends of temperature variations on the workpiece and the tool are different, especially at the beginning of the process, due to the time required for heat transfer from the workpiece to the die. At higher ironing speeds, the die is heated only in a narrow contact zone. In numerical experiments, the maximum temperature in the die was determined to be 133 °C. Numerical estimates of the temperature on the workpiece at a speed of 10000 mm/s, which corresponds to an industrial production of 250 cans per minute, give a maximum temperature value of 166 °C, which is still lower than the critical melting temperature of the tin coating, which is 232 °C. From the aforementioned concluding considerations, it is necessary to take into account the generated heat in the interface, especially at higher ironing speeds, and enable its removal from the contact zone using a lubricant that should also have the role of coolant.

Acknowledgements

The part of this research is supported by the Ministry of Science, Technological Development and Innovation, Republic of Serbia, Grant TR34002 and Grant TR32036.

6 REFERENCES

- [1] Stolte, E. (1962). Martensitbildung in der Oberfläche Kochlenstoffhaltiger Stähle aus Folge Kurzeitiger intensiver Gleitreibung. *Techn. Mitteil. Krupp*, 14.
- [2] Barber, J. R. (1967). The influence of thermal expansion on the friction and wear process. *Wear*, 12. [https://doi.org/10.1016/0043-1648\(67\)90087-7](https://doi.org/10.1016/0043-1648(67)90087-7)
- [3] Schünemann, M., Ahmetoglu, M. A., & Altan, T. (1996). Prediction of process conditions in drawing and ironing of cans. *Journal of Materials Processing Technology*, 59, 1-9. [https://doi.org/10.1016/0924-0136\(96\)02280-7](https://doi.org/10.1016/0924-0136(96)02280-7)
- [4] Üstünyagiz, A., Nielsen, C. V., Christiansen, P., Martins, P. A. F., & Altan, T. (2019). A combined numerical and experimental approach for determining the contact temperature in an industrial ironing operation. *Journal of Materials Processing Tech.*, 264, 249-258. <https://doi.org/10.1016/j.jmatprotec.2018.09.015>
- [5] Sauer, R. (1998). Abstreckgleitziehen Fertigung von Weißblechdosen. *Metall*, 52, 10-11.
- [6] Djordjević, M., Aleksandrović, S., Djačić, S., Sedmak, A., Lazić, V., Arsić, D., & Mutavdžić, M. (2019). Simulation of Flat Die Deep Drawing Process by Variable Contact Pressure Sliding Model. *Technical Gazette*, 26(5), 1199-1204. <https://doi.org/10.17559/TV-20161215205553>
- [7] Adamovic, D. (2002). *Materials behaviour in contact at processes of plastic deformation with high working pressures*. Doctoral thesis. The Faculty of Mechanical Engineering, University of Kragujevac, Serbia.
- [8] Kim, H., Altan, T., & Yan, Q. (2009). Evaluation of stamping lubricants in forming advanced high strength steels (AHSS) using deep drawing and ironing tests. *Journal of Materials Processing Technology*, 209, 4122-4133. <https://doi.org/10.1016/j.jmatprotec.2008.10.007>
- [9] Chandrasekharan, S., Palaniswamy, H., Jaina, N., Ngaile, G., & Altan, T. (2005). Evaluation of stamping lubricants at various temperature levels using the ironing test. *International Journal of Machine Tools & Manufacture*, 45, 379-388. <https://doi.org/10.1016/j.ijmactools.2004.09.014>
- [10] Nam, J. & Han, K. S. (2000). Finite Element Analysis of Deep Drawing and Ironing Process in the Steel D & I Canmaking. *ISIJ International*, 40(12), 1223-1229. <https://doi.org/10.2355/isijinternational.40.1223>
- [11] Singh, S. K., Kumara, V., Reddy, P. P., & Guptab, A. K. (2014). Finite element simulation of ironing process under warm conditions. *Journal of Mater. Res. Tech.*, 3(1), 7178. <https://doi.org/10.1016/j.jmrt.2013.10.013>
- [12] Adamovic, D., Mandic, V., Jurkovic, Z., Grizelj, B., Stefanovic, M., Mrinkovic, T., & Aleksandrovic, S. (2010). An experimental modelling and numerical FE analysis of steel-strip ironing process. *Technical Gazette*, 17(4), 435-444.
- [13] Mandić, V., Adamović, D., Jurković Z., Stefanović, M., Živković, M., Randelović, S., & Marinković, T. (2010). Numerical FE Modelling of the Ironing Process of Aluminium Alloy and its Experimental Verification. *Famena*, 34(4), 59-69.
- [14] Mandić, V. (2012). *Physical and numerical modelling of forming processes*. Faculty of Engineering, Serbia.
- [15] Simufact. *Simulating Forming with Simufact Forming*.
- [16] Serban, F. M., Grozav, S., Ceclan, V., & Turcu, A. (2020). Artificial Neural Networks Model for Springback Prediction in the Bending Operations. *Technical Gazette*, 27(3), 868-873. <https://doi.org/10.17559/TV-20141209182117>
- [17] Özdemir, M. & Gokmese, K. (2018). Microstructural Characterization and Deformation of X10CrAlSi24 Sheet Material Applied V-Bending Process. *Technical Gazette*, 25(3), 846-854. <https://doi.org/10.17559/TV-20170425022545>

Contact information:

Vesna MANDIĆ, Full professor
(Corresponding author)
Faculty of Engineering University of Kragujevac,
Sestre Janjić 6, 34000 Kragujevac, Republic of Serbia
E-mail: mandic@kg.ac.rs

Dragan ADAMOVIĆ, Full professor
Faculty of Engineering University of Kragujevac,
Sestre Janjić 6, 34000 Kragujevac, Republic of Serbia
E-mail: adam@kg.ac.rs

Zoran JURKOVIĆ, Full professor
Faculty of Engineering, University of Rijeka,
Vukovarska 58, 51000 Rijeka, Republic of Croatia
E-mail: zoran.jurkovic@riteh.hr

Marko DELIĆ, Teaching assistant
Faculty of Engineering University of Kragujevac,
Sestre Janjić 6, 34000 Kragujevac, Republic of Serbia
E-mail: marko.delic@kg.ac.rs